Unraveling the Compromise Between Skull Stripping and Inhomogeneity Correction in 3T MR Images

Fábio A.M. Cappabianco
Instituto de Ciência e Tecnologia
Universidade Federal de São Paulo
São José dos Campos, Brazil
cappabianco@unifesp.br

Paulo A.V. de Miranda
Institute of Mathematics and Statistics
University of São Paulo
São Paulo, Brazil
pmiranda@vision.ime.usp.br

Jaime S. Ide
Instituto de Ciência e Tecnologia
Universidade Federal de São Paulo
São José dos Campos, Brazil
jaime.ide@unifesp.br

Clarissa L. Yasuda
School of Medical Science
University of Campinas
Campinas, Brazil
yasuda.clarissa@gmail.com

Alexandre X. Falcão
Institute of Computing
University of Campinas
Campinas, Brazil
afalcao@ic.unicamp.br

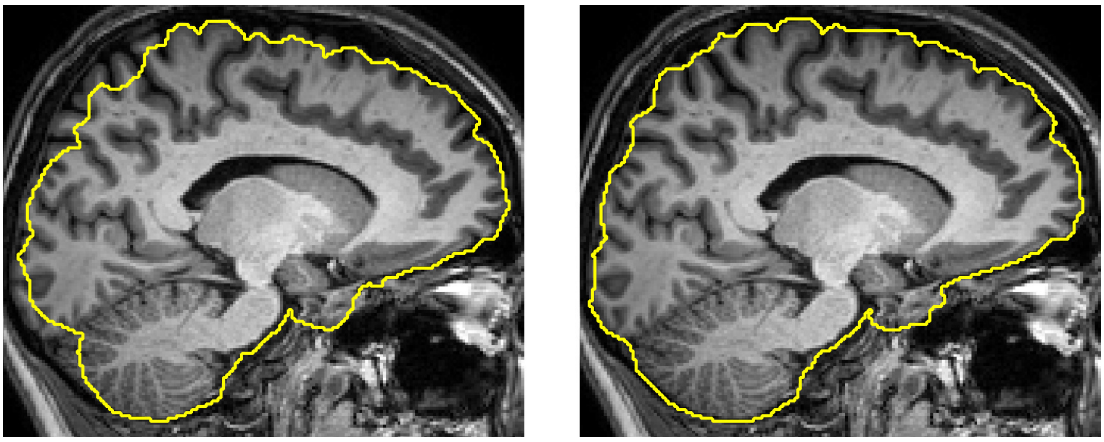

Fig. 1. Teasing the need for inhomogeneity correction prior to skull stripping in high magnetic resonance field images (e.g. 3 Tesla). Left: Segmentation made by a popular automatic method. Right: Improved skull stripping applying a novel proposed iterative inhomogeneity correction methodology.

***Abstract*—Bias field (inhomogeneity) correction and skull stripping are initial standard procedures in medical image analysis of the human brain. Several works have investigated the effects of prior inhomogeneity correction on skull stripping using 1.5 Tesla magnetic resonance (MR) images, but this question remains unanswered for higher magnetic fields. This paper fills this gap using 3 Tesla MR-images, by proposing a novel alternate sequence of skull stripping, morphological operations, inhomogeneity correction and intensity standardization, with the first at the beginning and end of the sequence, denominated Iterative Skull Stripping methodology. Conversely to what happens in 1.5T images, experimental evaluation shows that, in 3 Tesla datasets, inhomogeneity effect plays an important role in stripping the brain. This observation produces a deep impact on previous and future studies that rely on skull stripping operation.**

***Keywords*-Image Segmentation, Brain Magnetic Resonance Imaging, Inhomogeneity/Bias Correction, Standardization, Skull Stripping**

I. Introduction

Skull stripping and inhomogeneity (non-uniformity or bias field) correction are two important procedures that compose most of the frameworks in medical image analysis of the human brain [1], [2], [3], [4]. Recent reviews of bias field correction algorithms [5], [6], [7] analyzed the effects of skull stripping prior to the inhomogeneity correction in 3 Tesla (3T) images. For instance, [7] evaluated the Nonparametric Nonuniform intensity Normalization method [8] in a 3T database using different configurations. They concluded that bias field correction can be improved as long as a precise input brain mask is provided. However, the question whether prior inhomogeneity correction improves skull stripping in 3T images

remains open. Reviews about skull stripping methods [9], [10] restricted their bias field investigations to 1.5 Tesla MR datasets and synthetic images. For these MR modalities, authors in [10] concluded that inhomogeneity correction did not improve significantly the stripped brain in any condition.

This paper fills the gap of evaluating the influence of inhomogeneity over skull stripping methods in 3T MR-images. Our analysis shows that, in contrast to what happens in 1.5T and in synthetic images, some of the standard solutions underestimate brain tissues in the external cortical area and around the cerebellum.

Since inhomogeneity effects are stronger in higher magnetic fields, it is extremely important to define the optimal solution for this modality. In order to improve previous results of the standard state-of-art algorithms like Brain Extraction Tool [11], we propose a novel methodology denominated Iterative Skull Stripping (ISS) that extracts the brain by iteratively applying an alternate sequence of skull stripping, morphological operations, inhomogeneity correction, intensity standardization, and skull stripping.

In the rest of this paper, Section II describes the evaluated methods. The ISS solution is presented in Section III; Section IV contains the experimental analysis and results; finally, conclusions are summarized in Section V.

II. Methods description

In this section, we will briefly describe the evaluated methods. Brain Extraction Tool [11] (BET) is a popular skull stripping method. It uses the regional intensity properties to compute the driving forces that push a template outward. Robust regional image intensity minimum and maximum are obtained from the histogram by excluding intensity outliers. BET makes use of a nonlinear smoothness constraint on the deformable model.

Nonparametric Nonuniform intensity Normalization [8] (N3) is an up-to-date powerful technique for correcting the intensity inhomogeneity in MR-images. It achieves high performance without the construction of tissue intensity or geometric models beforehand. N3 uses a deconvolution kernel to correct the smoothing caused by the bias field, sharpening the intensity histograms. Distinctly from the majority of the other methods, N3 can be executed prior to skull stripping, since it does not require a brain delineation.

The method presented in [12] that we will refer to as Reference Voxel (RV) is a recent algorithm for inhomogeneity correction. It assumes that white matter (WM) voxels are not far from other brain voxels. Bias field is estimated based on relationships between global maximal intensity and local maxima restricted to an adaptive spherical adjacency centered in each voxel.

III. Iterative Skull Stripping methodology

We start this section by showing the differences and problems faced when stripping the brain in 1.5T and in 3T datasets. Although contrast between gray matter (GM) and WM tissues is improved in 3T, the gradient between GM and cerebral-spinal fluid (CSF) is weaker due to stronger bias field (Figure 2). It is expected that brain boundaries composed by such weaker edges are harder to be distinguished. Figure 3 shows common segmentation problems that arise when segmenting 3T images with BET and an alternative method called Clouds [13] with their standard parameters.

We can conclude from the presented analysis and previous studies [7] that inhomogeneity correction and skull stripping are mutually dependent tasks in 3T images. On one hand, most inhomogeneity correction methods require a brain mask as input. Bias field correction by N3 without the input mask is not as effective as we show in the experiments of Section IV. On the other hand, stripping the brain from the original image usually results in underestimation of the brain volume (Figure 3). To handle this circular reference problem, we propose the ISS solution that uses alternately any combination of methods for inhomogeneity correction and skull stripping, along with morphological operations and intensity standardization. First, ISS strips the brain from the original image just to have an estimation of the brain mask (Figure 4(a-c)). As the brain mask is underestimated, the mask is dilated and used as input to an inhomogeneity correction algorithm (Figure 4(d-e)). The complement of the dilated mask is computed, multiplied by the original image and added to the corrected brain (Figure 4(f-g). The combined image now has the brain region free from inhomogeneity effects and can be stripped again with more precision (Figure 4(h).

It is important to note that the corrected brain of Figure 4(e) may be standardized [14] to the source image domain. Standardization is specially important if the inhomogeneity correction method changes the range of the intensities since, the corrected brain restricted to the dilated mask from the first stripping operation is combined with the mask complement multiplied by the input image in order to restore the entire image domain.

Algorithm 1 summarizes the main ideas of ISS. In Lines 1 and 2, the iteration number and the current full image are initialized. Line 3 executes the first skull stripping required at the beginning of the process. The remaining code (Lines 3 to 12) is the main loop of the algorithm. When the last iteration is achieved (checked in Line 4), the execution is over, and the stripped brain is returned (Line 13). Lines 5 to 6 compute a binary brain mask and dilate it using mathematical morphology, to ensure that most of the brain is contained in the mask. Dilation may be performed or not based on the employed skull stripping method behavior. The current image, restricted to the dilated binary mask, is then corrected from bias effects (Line 7). After that, the corrected brain is standardized (Lines 8) and added to the complement mask of the dilated brain, multiplied by the original image (Line 9).Finally, iteration number is updated (Line 10), the brain is segmented from the composed image I (Line 11), and execution jumps back to Line 4.

Note that one might employ different parameters or even distinct skull stripping and inhomogeneity correction algorithms in each iteration. Also, instead of using a defined

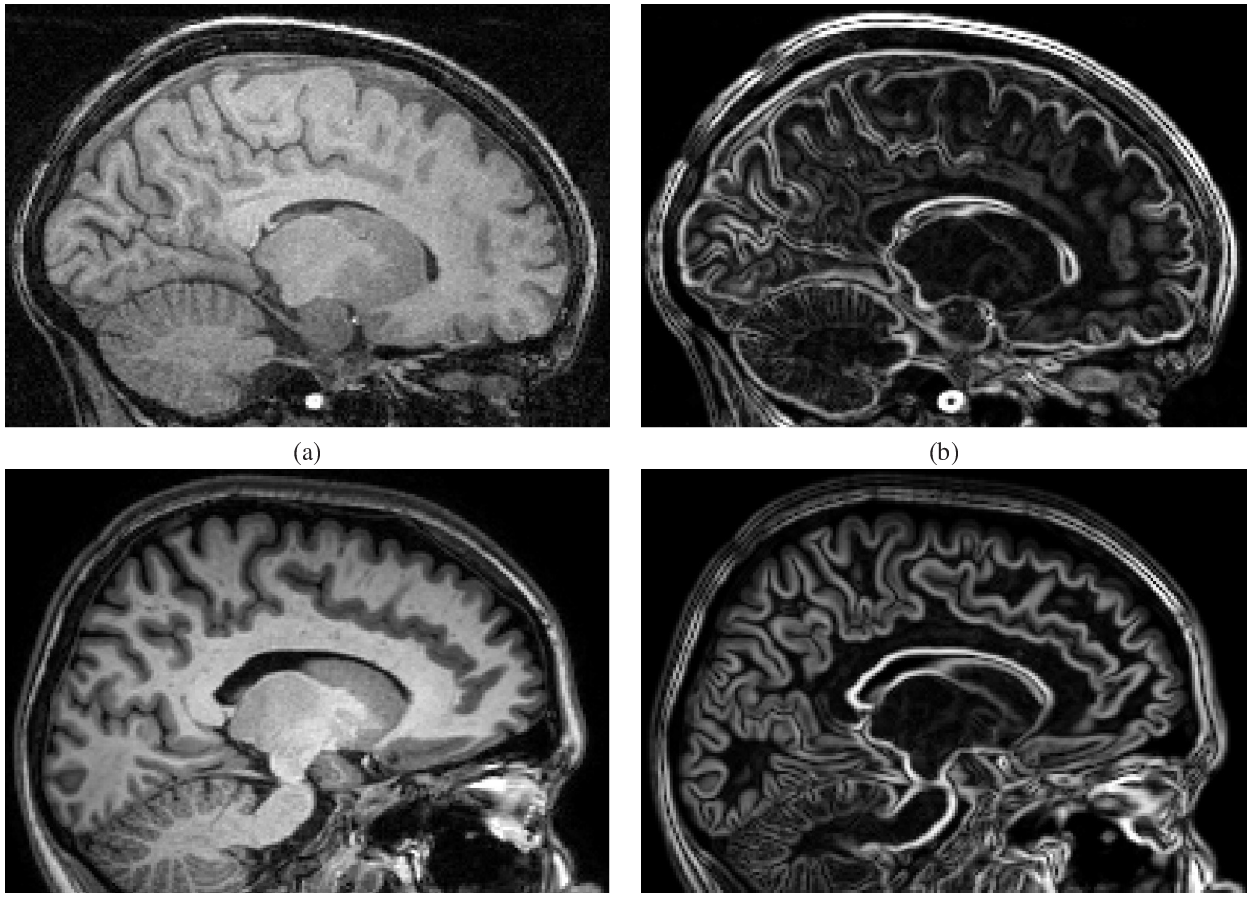

Fig. 2. (a) 1.5 Tesla image and (b) its gradient. (c) 3.0 Tesla image and (d) its gradient. Edges between CSF and dura matter, and between GM and CSF in the cortex region are clearer in 1.5 Tesla images.

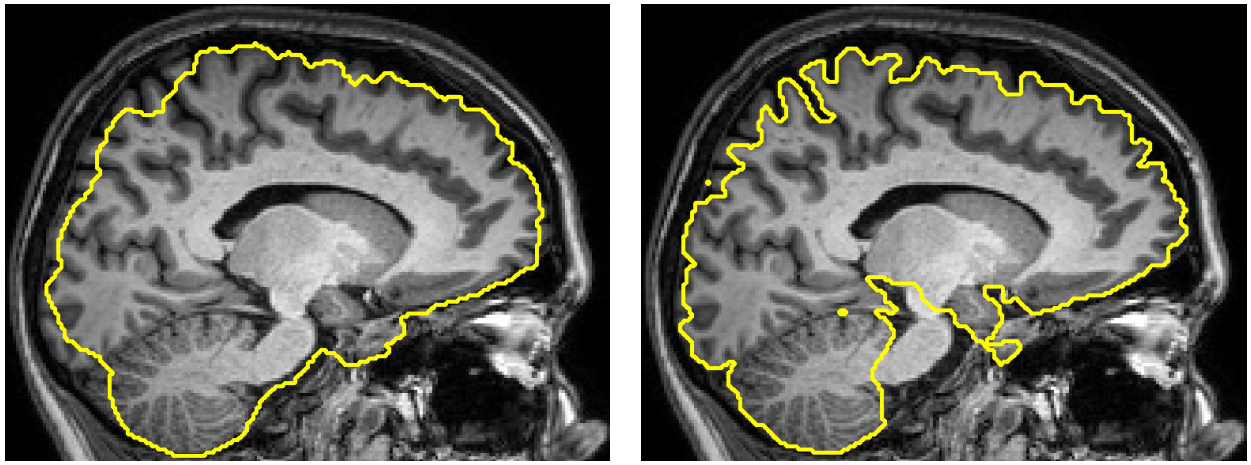

Fig. 3. (a) Brain segmented by BET. (b) Segmentation performed by Clouds. Input image is shown in Figure 2(c). Using standard parameters, both methods underestimated brain tissues.

number of iterations T, the user might stop execution when M is satisfactory, in a semi-automatic fashion. We observed that in practice, two iterations of the algorithm (i.e. $T = 2$) are enough to achieve good results.

IV. Experiments and Results

The following experiments elucidate the influence of single and iterative inhomogeneity correction over skull stripping in 3 Tesla database. For this purpose, we combine BET skull

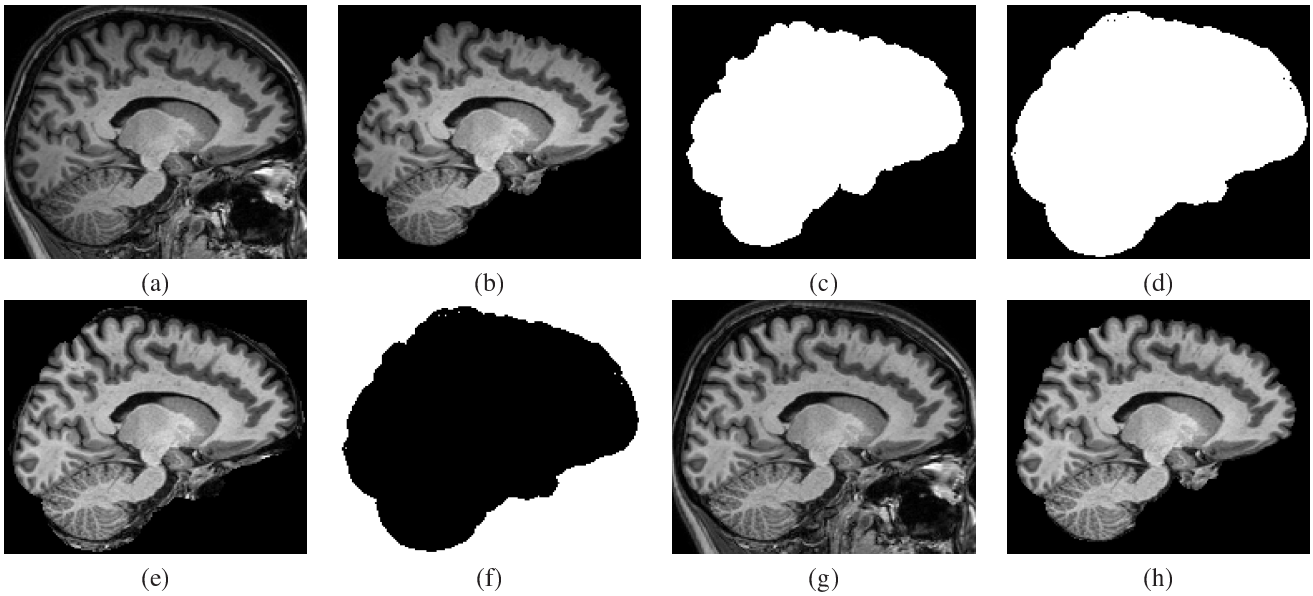

Fig. 4. Sample of ISS algorithm execution. The numbers inside quotation marks refer to the lines of algorithm 1. Intensity standardization is not showed here, since inhomogeneity correction did not change the original range. (a) Input brain sagittal slice. (b) First skull stripping "Line 3". (c) Binary brain mask "Line 5". (d) Dilated brain mask "Line 6". (e) Intensity correction of the input image restricted to the dilated mask "Line 7". (f) Binary mask containing the complement of the stripped brain "Line 9". (g) Addition of the corrected brain and the complement of the input brain "Line 9". (h) Final skull stripping from the image (g) "Line 11".

Algorithm 1: Iterative Skull Stripping

Inputs: Image I_0**, number of iterations** T.
Outputs: Stripped Brain M.
Auxiliary: Variable t**, temporary images** B, D, I, J, K, M.

1: $I \leftarrow I_0$.
2: $t \leftarrow 1$.
3: $M \leftarrow Brain(I)$.
4: **while** $t \neq T$ **do**
5: $B \leftarrow Binary(M)$.
6: $D \leftarrow Dilate(B)$. {**Optional. Use** $D \leftarrow B$ **if** B **is large enough.**}
7: $J \leftarrow Correction(I, D)$.
8: $K \leftarrow Standardize(J, I_0)$.
9: $I \leftarrow SUM(Complement(I_0, D), K)$.
10: $t \leftarrow t + 1$.
11: $M \leftarrow Brain(I)$.
12: **end while**
13: **Return** M.

stripping method with RV and N3 inhomogeneity correction procedures. To the best of our knowledge there is no public 3 Tesla database with skull stripping ground-truth. Therefore, we used a database composed by 10 T1-images of 3T. The individuals are males and females, from 24 to 53 years old, and they have normal brains. The scanner is a 3T scanner (Philips Achieva), - T1- weighted 3-dimension gradient echo with 1mm isotropic voxels, acquired in the sagittal plane (1mm thick, flip angle, 8; TR, 7.1; TE, 3.2; matrix, 240x240; e FOV, 240x240cm). Ground-truths (GTs) were manually delineated by a specialist.

Even though it is possible to achieve better results by ajusting the parameters of the skull stripping methods, sometimes this procedure is not practical. It takes time and requires extra effort of the user to evaluate several segmented images. For instance, in a population study containing hundreds of subjects it is unfeasible to analyze skull stripping results of each image with different parameters. In this case, one can choose default parameters or select the parameters based on a few samples. We ran several experiments over our dataset and observed that the best set of parameters differs for each image.

Therefore, we executed experiments using the default parameters of considered methods according to the expected and/or suggested settings given by the authors. For BET, we set the center of gravity manually, by using '-c' parameter, as suggested in FMRIB Software Library (FSL) website[1], because images have a large portion of the neck. BET parameter '-c' was set to 90 120 155. These coordinates correspond to Right-Left, Posterior-Anterior, and Inferior-Superior orientations, respectively.

First, skull stripping was performed in original images (BET). Than, we compared these results to BET skull stripping after inhomogeneity correction by N3 without brain mask input and default parameters (N3+BET). Then, we tested ISS methodology in the framework of Algorithm 1, employing two skull stripping iterations with the configurations: BET, followed by N3 and BET (ISS:BET+N3+BET), and BET, followed by RV and BET (ISS:BET+RV+BET). Both N3 and RV were executed with default parameters. We also tried to correct inhomogeneity using N3 without a brain mask input, prior to the first skull stripping, that is ISS:N3+BET+RV+BET and ISS:N3+BET+N3+BET, but it did not improve the results of ISS:BET+RV+BET and ISS:BET+N3+BET, respectively. ISS was tested with five different morphological dilation operations, using spherical kernel of radius 2.0mm, 3.0mm,

[1]http://www.fmrib.ox.ac.uk/fsl/

4.0mm, 5.0mm, and 6.0mm.

The best results for both ISS:BET+N3+BET and ISS:BET+RV+BET were achieved using a dilation with radius of $5mm$. Dilation by smaller radius usually underestimate the brain volume. Using larger radius, excessively increases the mask volume, reducing the effectiveness of the inhomogeneity correction algorithms. Therefore, we just present results of ISS using radius of 5mm. Table I summarizes the accuracy of the evaluated methodologies using the Dice metric [15] between each result and its respective GT. ISS:BET+N3+BET achieved the best results for most of the images, followed by ISS:BET+RV+BET, N3+BET, and BET.

Dice metric may be biased by a small differences as one voxel distance between the result and the GT. To achieve more robust result analysis [16], we also present in Tables II and III the mean Euclidean distance error and the mean Euclidean square distance error between the segmented and the ground-truth boundaries, respectively. The results corroborate with Dice metric evaluation that ISS:BET+N3+BET and ISS:BET+RV+BET are the best options for stripping the brain. It is specially interesting to note that ISS:BET+N3+BET and ISS:BET+RV+BET produced the best rates in all cases, 7 and 3, respectively, using square Euclidean distance metric, which assigns greater penalty to longer distances.

The differences among ISS:BET+N3+BET, N3+BET, BET with respect to the mean square Euclidean distance are all statistically significant according to pairwise t-tests with $p < 0.01$. The only statistically significant involving ISS:BET+RV+BET according to the same criteria relates to BET methodology.

TABLE I
DICE METRIC ACCURACY OF BET SKULL STRIPPING (IN PERCENT). CELLS CONTAIN MEAN VALUES OF BET, N3+BET, ISS:BET+RV+BET, AND ISS:BET+N3+BET BY ISS METHODOLOGY. HIGHER VALUES INDICATE BETTER RESULTS. THE BEST RESULTS ARE IN RED.

Image	BET	N3+BET	ISS: BET+RV+BET	ISS: BET+N3+BET
0	95.18	95.38	95.27	95.67
1	94.19	94.88	96.39	96.30
2	94.00	94.51	94.85	95.17
3	94.32	94.72	95.17	95.30
4	94.59	95.49	95.72	95.81
5	95.15	95.43	95.50	95.58
6	95.49	95.62	95.43	95.78
7	93.96	94.12	94.72	94.76
8	94.49	94.70	94.93	95.08
9	94.63	95.24	94.83	95.50
Mean	94.60	95.01	95.27	95.50

Figures 5 to 7 show qualitative results in sagittal, coronal, and axial slices of the brain, respectively. In Figure 5, ISS:BET+RV+BET segmented the anterior superior part of the parietal lobe with more precision than the other methodologies. The same can be said about the left and right portion of the cerebellum in Figure 6. In Figure 7, on the other hand, ISS:BET+N3+BET significantly improved the results of BET segmentation all around the cortical region. Therefore, inhomogeneity correction improvements are remarkable. We

TABLE II
MEAN EUCLIDEAN DISTANCE METRIC ACCURACY OF BET SKULL STRIPPING (IN PERCENT). CELLS CONTAIN MEAN VALUES OF BET, N3+BET, ISS:BET+RV+BET, AND ISS:BET+N3+BET BY ISS METHODOLOGY. LOWER VALUES INDICATE BETTER RESULTS. THE BEST RESULTS ARE IN RED.

Image	BET	N3+BET	ISS: BET+RV+BET	ISS: BET+N3+BET
0	1.49	1.42	1.41	1.33
1	2.18	2.02	1.46	1.51
2	1.77	1.62	1.54	1.47
3	1.68	1.57	1.40	1.37
4	1.80	1.53	1.41	1.39
5	1.76	1.65	1.53	1.52
6	1.54	1.52	1.57	1.44
7	1.89	1.85	1.69	1.67
8	1.68	1.59	1.54	1.49
9	1.74	1.58	1.64	1.48
Mean	1.75	1.64	1.52	1.47

TABLE III
MEAN SQUARE EUCLIDEAN DISTANCE METRIC ACCURACY OF BET SKULL STRIPPING (IN PERCENT). CELLS CONTAIN MEAN VALUES OF BET, N3+BET, ISS:BET+RV+BET, AND ISS:BET+N3+BET BY ISS METHODOLOGY. LOWER VALUES INDICATE BETTER RESULTS. THE BEST RESULTS ARE IN RED.

Image	BET	N3+BET	ISS: BET+RV+BET	ISS: BET+N3+BET
0	3.57	3.15	3.12	2.65
1	8.17	6.99	3.39	3.64
2	5.30	4.29	3.76	3.45
3	4.53	3.86	2.74	2.58
4	5.45	3.62	2.83	2.71
5	5.10	4.42	3.38	3.40
6	3.58	3.49	3.54	2.92
7	6.52	6.31	4.52	4.69
8	4.35	3.81	3.37	3.16
9	5.02	3.98	4.25	3.39
Mean	5.16	4.39	3.49	3.26

repeated these qualitative experiments with more than 20 3T images, and the results were similar.

The main drawback of ISS methodology is its relatively higher computational cost. The execution time T_1 of the traditional approach composed by inhomogeneity correction and skull stripping is given by

$$T_1 = T_I + T_S, \quad (1)$$

where T_S and T_I are the execution times of the skull stripping and inhomogeneity correction algorithms, respectively. Using ISS with one iteration, the execution time T_{ISS} is given by

$$T_{ISS} = T_I + 2T_S + T_D + T_A + T_P, \quad (2)$$

where T_D, T_A, and T_P are the execution times of the binary morphological dilation, intensity standardization, and the voxel-based image operations (i.e. addition, complement, and multiplications), respectively. Therefore, we have:

$$T_{ISS} = T_1 + T_S + T_D + T_A + T_P. \quad (3)$$

In practice, T_I may be different in Equations 1 and 2, since the inhomogeneity correction is applied to the entire image in the first case, and in the second it is restricted to the dilated

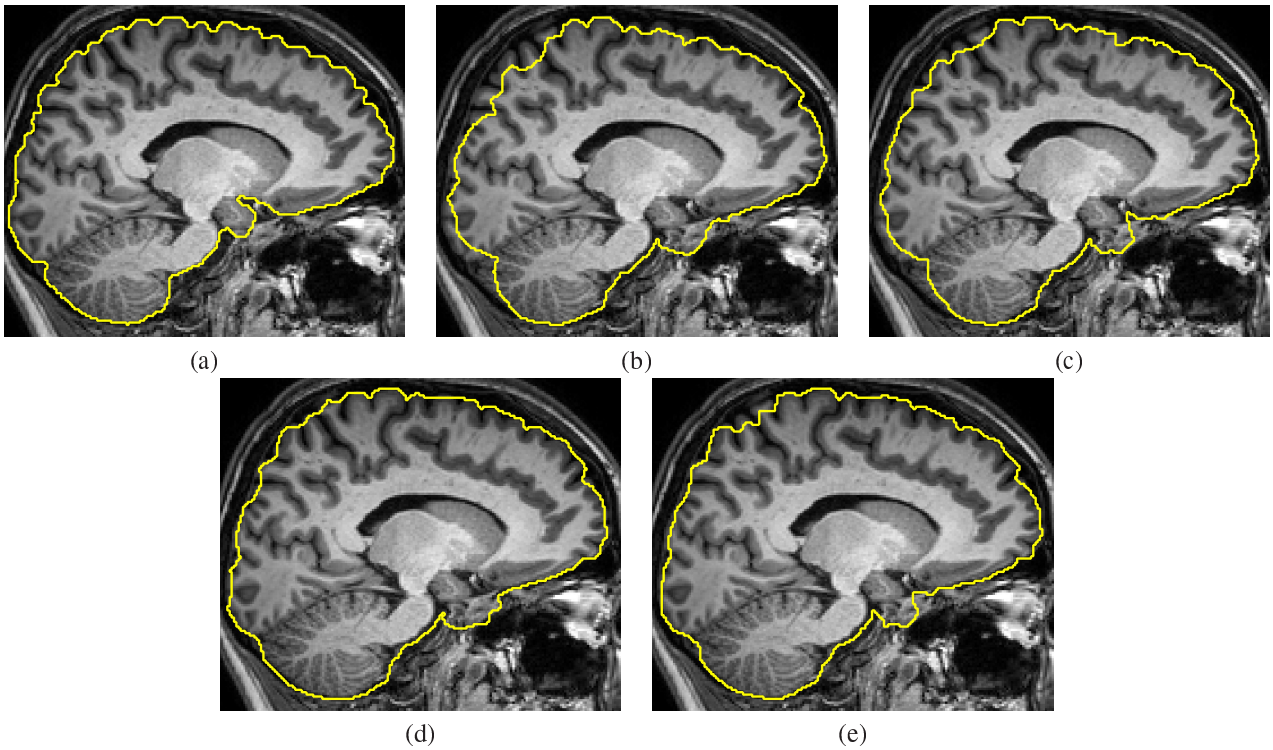

Fig. 5. Results of skull stripping with default parameters in a sagittal slices of image 1 from the quantitative experiments performed by methodologies: (a) Manual segmentation, (b) BET, (c) N3+BET, (d) ISS:BET+RV+BET, and (e) ISS:BET+N3+BET.

brain. This is the case of N3 as it is used in N3+BET and ISS:BET+N3+BET approaches (e.g. Image 4 in Table IV). Table IV displays the single-thread execution time of each methodology over our dataset. The tests were executed in an Intel Core i5-2400 PC, with 4GB of memory.

TABLE IV
EXECUTION TIME OF BET SKULL STRIPPING IN SECONDS. CELLS CONTAIN MEAN VALUES OF BET, N3+BET, ISS:BET+RV+BET, AND ISS:BET+N3+BET BY ISS METHODOLOGY. LOWER VALUES INDICATE BETTER RESULTS.

Image	BET	N3+BET	ISS: BET+RV+BET	ISS: BET+N3+BET
0	4.01	15.31	19.95	22.44
1	4.00	17.46	20.65	24.83
2	3.90	19.72	19.55	23.74
3	4.05	16.86	21.74	26.01
4	4.28	28.98	22.15	30.43
5	3.86	19.58	19.33	24.55
6	4.76	16.94	23.25	27.09
7	4.76	23.29	23.09	30.24
8	4.28	18.43	21.04	25.02
9	4.32	25.61	20.62	27.26
Mean	4.22	20.21	21.13	26.16

V. CONCLUDING REMARKS

The main contribution of this paper is showing that, in 3T datasets, inhomogeneity effect plays an important role while stripping the brain, contrarily to what happens is 1.5T images. To the best of our knowledge, this is the first study demonstrating the inhomogeneity influence over skull stripping algorithms using a 3T MR database. This observation produces a deep impact on previous and future studies that rely on skull stripping operation.

After noting that the combination N3+BET provides better results than skull stripping with no bias-field correction, we also propose an iterative methodology to correct inhomogeneity at the same time that brain is stripped and standardized, called ISS. Even though ISS demands higher execution time, it proved to be simple, accurate, and versatile, because it can virtually use any combination of methods for inhomogeneity correction and skull stripping.

There are several popular inhomogeneity correction and skull stripping methods such as Brain Surface Extractor and Bias Field Corrector [17] from BrainSuite[2] framework; Hybrid Watershed Algorithm (HWA) [18] contained in Freesurfer[3]; and Clouds [13] among others. We will consider them and more extensive evaluations in future works.

ACKNOWLEDGMENT

The authors would like to thank Fapesp(2011/08753-4) and CNPQ for financial support.

REFERENCES

[1] M. Bondi, W. Houston, L. Eyler, and G. Brown, "fmri evidence of compensatory mechanisms in older adults at genetic risk for alzheimer disease," *Neurology*, vol. 64, no. 3, pp. 501–508, 2005.

[2] J. Acosta-Cabronero, G. Williams, J. Pereira, G. Pengas, and P. Nestor, "The impact of skull-stripping and radio-frequency bias correction on grey-matter segmentation for voxel-based morphometry," *Neuroimage*, vol. 39, no. 4, pp. 1654–1665, 2007.

[2]http://www.loni.ucla.edu/Software/BrainSuite

[3]http://surfer.nmr.mgh.harvard.edu/

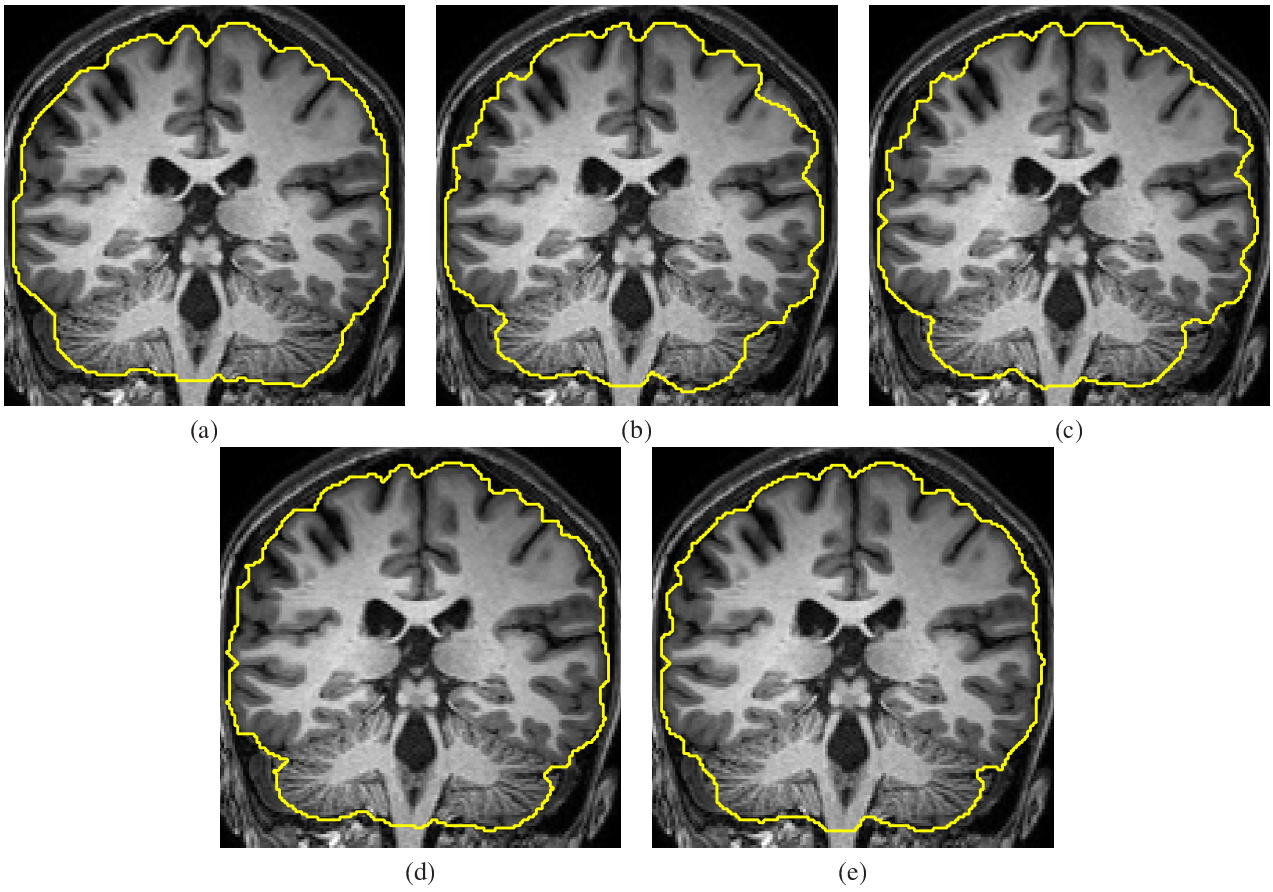

Fig. 6. Results of skull stripping with default parameters in a coronal slices of image 1 from the quantitative experiments performed by methodologies: (a) Manual segmentation, (b) BET, (c) N3+BET, (d) ISS:BET+RV+BET, and (e) ISS:BET+N3+BET.

[3] R. Desikan, H. Cabral, B. Fischl, C. Guttmann, D. Blacker, B. Hyman, M. Albert, and R. Killiany, "Temporoparietal mr imaging measures of atrophy in subjects with mild cognitive impairment that predict subsequent diagnosis of alzheimer disease," *American Journal of Neuroradiology*, vol. 30, no. 3, pp. 532–538, 2009.

[4] J. Acosta-Cabronero, G. Williams, G. Pengas, and P. Nestor, "Absolute diffusivities define the landscape of white matter degeneration in alzheimer's disease," *Brain*, vol. 133, no. 2, pp. 529–539, 2010.

[5] J. Arnold, J. Liow, K. Schaper, J. Stern, J. Sled, D. Shattuck, A. Worth, M. Cohen, R. Leahy, J. Mazziotta, and D. Rottenberg, "Qualitative and quantitative evaluation of six algorithms for correcting intensity nonuniformity effects," *NeuroImage*, vol. 13, no. 5, pp. 931–943, 2001.

[6] U. Vovk, F. Pernus, and B. Likar, "A review of methods for correction of intensity inhomogeneity in MRI," *IEEE Transactions on Medical Imaging*, vol. 26, no. 3, pp. 405–421, 2007.

[7] R. Boyes, J. Gunter, C. Frost, A. Janke, T. Yeatman, D. Hill, M. Bernstein, P. Thompson, M. Weiner, N. Schuff *et al.*, "Intensity nonuniformity correction using n3 on 3-t scanners with multichannel phased array coils," *Neuroimage*, vol. 39, no. 4, pp. 1752–1762, 2008.

[8] J. Sled, A. Zijdenbos, and A. Evans, "A nonparametric method for automatic correction of intensity nonuniformity in MRI data," *IEEE Transactions on Medical Imaging*, vol. 17, no. 1, pp. 87–97, 1998.

[9] K. Boesen, K. Rehm, K. Schaper, S. Stoltzner, R. Woods, E. Luders, and D. Rottenberg, "Quantitative comparison of four brain extraction algorithms," *NeuroImage*, vol. 22, no. 3, pp. 1255–1261, 2004.

[10] C. Fennema-Notestine, I. Ozyurt, C. Clark, S. Morris, A. Bischoff-Grethe, M. Bondi, T. Jernigan, B. Fischl, F. Segonne, D. Shattuck, R. Leahy, D. Rex, A. Toga, K. Zou, M. BIRN, and G. Brown, "Quantitative evaluation of automated skull-stripping methods applied to contemporary and legacy images: Effects of diagnosis, bias correction, and slice location," *Human brain mapping*, vol. 27, no. 2, pp. 99–113, 2006.

[11] S. Smith, "Fast robust automated brain extraction," *Human Brain Mapping*, vol. 17, no. 3, pp. 143–155, 2002.

[12] F. Cappabianco, J. Udupa, G. Araujo, and A. Falcão, "Brain Tissue MR-Image Segmentation via Optimum-Path Forest Clustering," in *Workshops of Sibgrapi 2011 - Theses and Dissertations*, D. M. Adelailson Peixoto and T. Vieira, Eds. Maceió, AL: SBC, august 2011, pp. 19–24. [Online]. Available: http://www.im.ufal.br/evento/sibgrapi2011/

[13] P. Miranda, A. Falcão, and J. Udupa, "Cloud bank: A multiple clouds model and its use in MR brain image segmentation," in *IEEE ISBI*, June 2009, pp. 506–509.

[14] A. Madabhushi and J. Udupa, "Interplay between intensity standardization and inhomogeneity correction in MR image processing," *IEEE Transactions on Medical Imaging*, vol. 24, no. 5, pp. 561–576, 2005.

[15] L. Dice, "Measures of the amount of ecologic association between species," *Ecology*, vol. 26, pp. 297–302, 1945.

[16] J. Udupa, V. LeBlanc, Y. Zhuge, C. Imielinska, H. Schmidt, L. Currie, B. Hirsch, and J. Woodburn, "A framework for evaluating image segmentation algorithms," *Computerized Medical Imaging and Graphics*, vol. 30, no. 2, pp. 75–87, 2006.

[17] D. Shattuck, S. Sandor-Leahy, K. Schaper, D. Rottenberg, and R. Leahy, "Magnetic resonance image tissue classification using a partial volume model," *NeuroImage*, vol. 13, no. 5, pp. 856–876, 2001.

[18] F. Segonne, A. Dale, E. Busa, M. Glessner, D. Salat, H. Hahn, and B. Fischl, "A hybrid approach to the skull stripping problem in MRI," *Neuroimage*, vol. 22, no. 3, pp. 1060–1075, 2004.

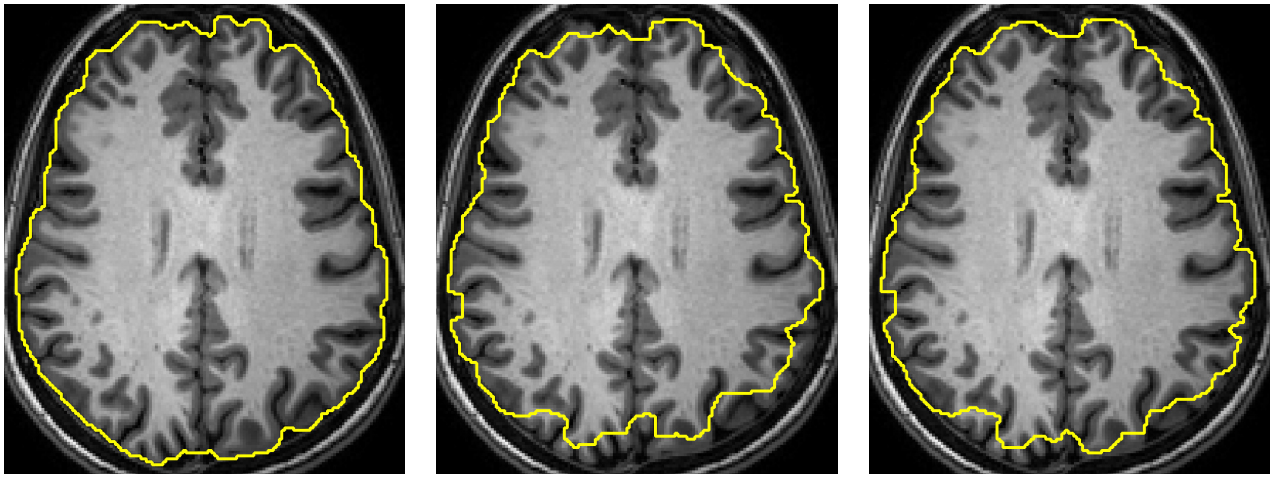

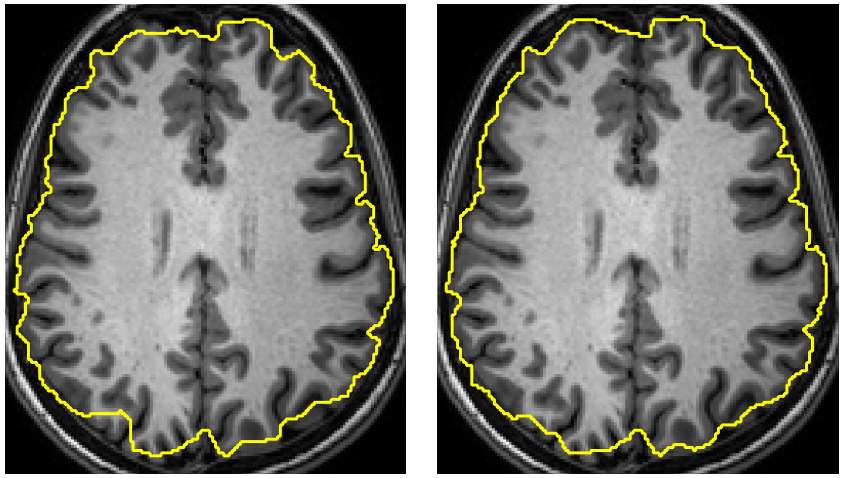

Fig. 7. Results of skull stripping with default parameters in a axial slices of image 1 from the quantitative experiments performed by methodologies: (a) Manual segmentation, (b) BET, (c) N3+BET, (d) ISS:BET+RV+BET, and (e) ISS:BET+N3+BET.